Structure optimization effects on the electronic and vibrational properties of $Bi_2Sr_2CaCu_2O_8$

V. Bellini* and F. Manghi
INFM-National Research Center on nanoStructures and bioSystems at Surfaces (S3) and Dipartimento di Fisica, Università di Modena e Reggio Emilia, Via Campi 213/A, I-41100 Modena, Italy

T. Thonhauser
Department of Physics, The Pennsylvania State University, University Park, Pennsylvania 16802, USA

C. Ambrosch-Draxl
Institut für Theoretische Physik, Universität Graz, Universitätsplatz 5, A-8010 Graz, Austria
(Received 21 July 2003; revised manuscript received 9 January 2004; published 26 May 2004)

We have studied the effect of structure optimization on the topology of the Fermi surface and on the Raman-active phonons of $Bi_2Sr_2CaCu_2O_8$. By total energy and force minimizations within the density-functional theory we have identified the most stable atomic geometry considering both an idealized body-centered tetragonal structure, inclusive of surface truncation, and a $\sqrt{2}\times\sqrt{2}$ orthorhombic cell simulating the observed distortions in the BiO planes. The optimization of the tetragonal cell leads to small but visible changes in the topology of the Fermi surface, rounding the shape of the CuO_2 barrels, while the orthorhombic distortion is responsible for the "umklapp" bands that have been observed by angle-resolved photoemission spectroscopy. The latter also gives rise to Raman-active vibrations not permitted in the tetragonal cell and strongly influences the attribution of the phonon peaks measured by experiments.

DOI: 10.1103/PhysRevB.69.184508 PACS number(s): 74.25.Kc, 74.25.Jb, 74.72.Hs, 71.15.Mb

I. INTRODUCTION

Among the high temperature superconductor (HTSC) cuprates the two-layer compound of the bismuth family, i.e., $Bi_2Sr_2CaCu_2O_8$ (Bi-2212), is a prototype for spectroscopic studies due to the relative ease to characterize a stable crystalline surface not exposed to segregation or oxygen depletion phenomena.[1] A thorough comparison between experimental data and theoretical calculations has been hindered up to now by the complex structure of this compound that makes the *ab initio* determination of electronic states a difficult task. Bi-2212 exhibits in fact an incommensurate superstructure[2–4] in the Bi-O plane, near to a commensurate orthorhombic distorted cell $\sqrt{2}\times 5\sqrt{2}$ with axes at 45° with respect to the in-plane Cu-O bonds. This distortion involves atomic displacements as large as 0.5 Å that are expected to affect the electronic bands.

A detailed knowledge of the low-energy electron excitations and the Fermi surface topology is essential to understand the unusual properties of the normal state of high-T_c cuprates and to shed light on the superconducting mechanism. A comparison between theoretical and experimentally determined Fermi surfaces requires a high level of accuracy in the computation of electronic states and various nontrivial ingredients such as (i) a realistic description of the complex crystal geometry and composition of the material in exam, inclusive of surface effects; (ii) many-body correlations associated to the strong interaction between localized electrons;[5] (iii) an explicit simulation of the photoemission process and of photoemission matrix elements. Most of the published works rely on drastic simplifications of some of these ingredients. All the first-principles band-structure calculations of Bi-2212 available up to now have been performed in an idealized crystal structure,[6–9] with lattice parameters taken from experiments and no optimization of the volume and atomic coordinates. These calculations predict BiO pockets around the *M* symmetry point in the Brillouin zone (BZ) that have no clear counterpart in the photoemission spectra;[10] moreover, the overall shape of the two main barrels centered at *X* is not correctly reproduced. Recently, it has been shown that the differences in the Fermi surface maps of Bi-2212 observed under various experimental conditions can be reproduced by the proper inclusion of photoemission matrix elements;[11,12] these calculations assumed however a perfect tetragonal structure and artificially modified the ionic potential to remove the BiO pockets around the M point.

In this paper, we focus on the effects induced on the low-energy excitations of Bi-2212 and on Raman-active phonons by a more accurate description of the geometrical structure. It has been demonstrated that the optimization of the crystal parameters (volume, c/a ratio, and atomic coordinates) leads in $YBa_2Cu_3O_7$ to a better agreement with experiments.[13] In the case of Bi-2212 we have to include also the Bi-O modulation occurring in the observed incommensurate superstructure. We do this adopting an averagely distorted orthorhombic (AD-ORTH) structure previously proposed for another compound of the bismuth family, i.e., the one CuO_2 plane compound Bi-2201.[14] By total-energy minimization we determine the equilibrium positions of the atoms considering both the ideal body-centered tetragonal (BCT) structure and the distorted one (AD-ORTH), and including also surface effects. As a severe test for the structures we calculate Raman-active phonon frequencies and eigenvectors and compare them with experimental data. There has been a renewed interest in the electron-phonon coupling as a non-

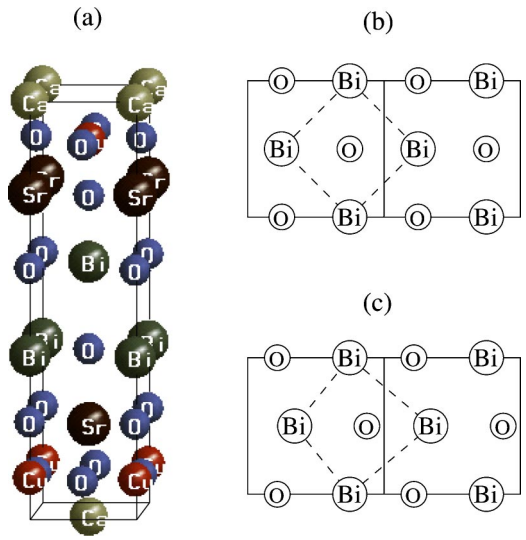

FIG. 1. (Color online) In (a) half of the primitive unit of the body-centered tetragonal (BCT) cell with space group $I4/mmm$ of Bi-2212 is depicted. In (b) and (c) the BiO plane is sketched in absence or presence of the distortion, respectively. The orthorhombic cell is rotated by 45° in the ab plane with respect to tetragonal one.

negligible and ubiquitous effect influencing the electron dynamics in the high-temperature superconductors;[15] accurate *ab initio* calculations of phonon modes are therefore very much needed, which were lacking for Bi compounds until now.

The work was organized as follows. After a brief introduction of the Bi-2212 crystal structure in Sec. II, the method in use and some computational details are presented in Sec. III. The discussion of the results will be addressed in Sec. IV, and conclusions will follow.

II. CRYSTAL STRUCTURE: BCT VS AD-ORTH

The basic unit of Bi-2212 is composed of two CuO_2 planes per cell separated by Ca ions, and two Bi-O layers separated from each of the CuO complexes by a Sr-O layer. The Bi-O planes have, similar to the Cu-O chains in the yttrium family, the role of a ''charge reservoir,'' attracting electrons and therefore doping the CuO_2 planes with holes. When the complex superstructures in the BiO plane observed by diffraction experiments are neglected, the crystal structure of Bi-2212 is well represented by the body-centered tetragonal cell (with space group *I4/mmm*) shown in Fig. 1(a). The superstructure arises because of the mismatch between the equilibrium Bi-O bond length and the lattice constant imposed by the CuO_2 planar nets. The weak coupling of the two BiO planes has been found to favor the appearance of such distortion, as opposed to the case of the Tl-2212 compound, where the shorter distance between the TlO planes is responsible for its absence. Moreover, the observed superstructure is incommensurate with respect to the Cu-O lattice constant, and is only approximately arranged by a $\sqrt{2} \times 5\sqrt{2}$ orthorhombic cell.[2] The full account of these distortions represents a severe task even for modern computers, as far as first-principles calculations are concerned. We have therefore chosen a more simplistic approach, considering the average displacements of the atoms from their tetragonal positions. Insets (b) and (c) in Fig. 1 show how the displacements of the O_{Bi} and Bi atoms in the BiO planes, allowed by an orthorhombic $\sqrt{2} \times \sqrt{2}$ cell (with space group *Bbmb*), account for the mean expansion and contraction of the Bi-O bonds. The type of distortion is the same assumed by Singh and Pickett[14] for the one-layer Bi-2201 compound, whereas we stress that for the Bi-2201 crystal the $\sqrt{2} \times \sqrt{2}$ cell itself is the commensurate analog to the real incommensurate superstructure. Here, it suffices to say that in-plane average displacements of around 0.5 Å (0.14 Å) along the distortion direction are observed for the O_{Bi} (Bi, O_{Sr}) atoms.[3] More details on the experimental lattice parameters as well as planar and off-plane coordinates of all the atoms in the BCT and AD-ORTH cells will be given later in the paper.

III. METHOD AND COMPUTATIONAL DETAILS

All calculations have been carried out using the full-potential linearized augmented plane-wave (LAPW) method[16,17] and its recent extension (APW+local orbital) as implemented in the WIEN2K code.[18] The muffin-tin radii inside which the plane waves are augmented by radial functions expanded over spherical harmonics have been chosen to be 1.9 (Ca), 1.9 (Cu), 2.2 (Sr), 2.25 (Bi), and 1.45 (O) Bohr. Exchange and correlation effects are accounted for by the local-density approximation (LDA). In the wave-function expansion $\approx$2200 (2400) basis functions have been used, and 40 (27) special **k** points within the irreducible part of the BZ sufficed for BZ integrations for the BCT (AD-ORTH) structure. Starting from the experimental parameters we have optimized the volume and c/a ratio for the BCT (and also b/a for the AD-ORTH) cell by minimization of the total energy. At each step the atoms were allowed to relax to their equilibrium positions under the influence of the atomic forces, a procedure leading to very accurate equilibrium structures. The remanent forces in this case are less than 0.2 mRy/a.u., which is an important starting point for the calculation of reliable phonon frequencies. Within the frozen-phonon approach a polynomial fit of calculated atomic-force values is carried out. For the fully symmetric A_g modes this was done for the equilibrium position plus two to four different displacements of each participating atom along the Cartesian axis. Diagonalization of the dynamical matrix yields the phonon frequencies as well as the normal vectors of the vibrations.

IV. RESULTS

A. Structural optimization

Starting from the experimental data by Sunshine *et al.*[19] (Exp) we have optimized the volume (Vol-Opt) or both, volume and c/a ratio (Full-Opt), as described above. The case where internal coordinates are relaxed using the experimental lattice volume and c/a ratio (Atom-Opt) is also given.

The results obtained using the BCT cell are reported in Table I; the well-known LDA underestimate of the volume is

TABLE I. Lattice parameters and atomic coordinates (in units of lattice constants) for the BCT structure of Bi-2212: columns 1–3 refer to different optimization levels (see text for the details), while in the last column the experimental data taken from Ref. 19 are listed.

	Full-Opt	Vol-Opt	Atom-Opt	Exp
Vol (Å^3)	202.2	202.2	226.3	226.3
c/a	8.258	8.065	8.065	8.065
$\Delta(E)$(mRy)	−67.4	−65.1	0	
z_{Cu}	0.0499	0.0498	0.0491	0.0543
z_{Sr}	0.1100	0.1103	0.1058	0.1091
z_{Bi}	0.2008	0.2015	0.1949	0.1989
$z_{\mathrm{O_{Cu}}}$	0.0514	0.0513	0.0503	0.0510
$z_{\mathrm{O_{Sr}}}$	0.1331	0.1328	0.1296	0.1200
$z_{\mathrm{O_{Bi}}}$	0.1991	0.2000	0.1929	0.1980

also found here and amounts to more than 10% [theory: 202.2 Å,[3] experiment 226.3 Å (Ref. 3)], while for (YBCO) it was around 6% only. The optimized c/a ratio is 2% larger than the experimental one, but its influence on the cohesive energy and the equilibrium positions of the nuclei is small. The calculated band structure for the experimental cell agrees very well with other LAPW results,[6,7] and will not be given here. Both the volume reduction and the increase in the c/a ratio results in a squeezing of the Cu-O in-plane bond length; as a net effect hybridization between CuO_2 and BiO planes through the SrO plane is favored inducing both BiO bands to cross the Fermi level. This is consistent with the results obtained by Szpunar and Smith in Ref. 9, who investigated the effect of stress along the c axis by decreasing the c/a ratio up to 12%, and found consistently the opposite trend, i.e., the BiO bands move to lower energies. For what concerns the atomic coordinates within the cell, a relevant change is the sizable increase of the dimpling in the SrO plane (of around 0.3 Å), while it is only slightly reduced in the CuO_2 and BiO planes. The dimpling of the CuO_2 plane in HTSC has been shown to be connected to the bifurcation of the saddle point near the $\bar{M}$ point,[20] and much attention has been devoted to it in the framework of the van Hove scenario.[21]

The same optimization procedure has been used for the AD-ORTH cell and the results are shown in Table II. Note that the the origin of the cell is shifted by $(a/2,b/2,-c/4)$ from the one of the BCT cells, while the orthorhombic x and y axes are rotated by 45° with respect to the tetragonal cell and point along the Bi-O bond directions. Compared to the BCT cell, a smaller reduction of the volume is found by LDA (4.2% vs 10%); the c/a (b/a) ratio increases (decreases) by about 2 (3.4)%. The atomic z coordinates are generally very similar to the ones in the BCT cell, while only a slight en-

TABLE II. Lattice parameters and atomic coordinates (in unit of lattice constants) for the AD-ORTH structure of Bi-2212: the experimental data are taken from Ref. 3.

	Full-Opt	Vol-Opt	Atom-Opt	Exp
Vol (Å^3)	428.1	428.1	446.7	446.7
c/a	5.827	5.711	5.711	5.711
b/a	0.963	$\simeq 1$	$\simeq 1$	$\simeq 1$
$\Delta(E)$(mRy)	−52.4	−35.2	0	
z_{Cu}	0.2019	0.2013	0.2011	0.1978
z_{Sr}	0.1441	0.1435	0.1445	0.1405
z_{Bi}	0.0543	0.0528	0.0542	0.0525
$z_{\mathrm{O^1_{Cu}}}$	0.1995	0.1991	0.1991	0.1976
$z_{\mathrm{O^2_{Cu}}}$	0.2006	0.2002	0.2002	0.1994
$z_{\mathrm{O_{Sr}}}$	0.1192	0.1192	0.1193	0.1189
$z_{\mathrm{O_{Bi}}}$	0.0568	0.0554	0.0571	0.0500
x_{Cu}	0.2497	0.2497	0.2496	0.2506
x_{Sr}	0.2526	0.2524	0.2536	0.2500
x_{Bi}	0.2269	0.2255	0.2202	0.2258
$x_{\mathrm{O^1_{Cu}}}$ [a]	0.0000	0.0000	0.0000	0.0012
$x_{\mathrm{O^2_{Cu}}}$ [a]	0.5000	0.5000	0.5000	0.4993
$x_{\mathrm{O_{Sr}}}$	0.2666	0.2663	0.2675	0.2750
$x_{\mathrm{O_{Bi}}}$	0.1705	0.1726	0.1703	0.1561

[a]The O_{Cu} atoms retain their tetragonal positions in our calculations.

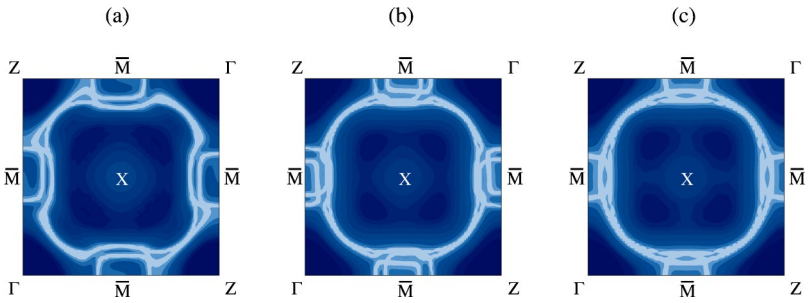

FIG. 2. (Color online) Fermi surface cross cuts in the k_x-k_y plane ($k_z=0$) for the BCT cell with (a) experimental and (b) optimized lattice constants and atomic positions (see Table I). (c) The same as in (b), but in the presence of a BiO terminated (001) surface, where the atomic positions were further relaxed in order to account for the breaking of the bonds at the surface layer.

hancement of the dimpling in SrO plane is found. As depicted in Fig. 1, the average displacements from the tetragonal positions of the Bi and O atoms in the BiO layers induce alternately expanded and contracted Bi-O bond distances along the x direction, which amount to 2.69 ± 0.64 Å and 2.67 ± 0.55 Å for the experimental and fully optimized structures, respectively. Along the other bond direction, which is now distorted into a zigzag line, the average bond distances are 2.72 Å and 2.59 Å for the experimental and optimized cells, respectively. Total energy calculations performed with the experimental lattice constants show that the distorted structure is more stable than the tetragonal one with an energy difference of 0.60 eV per formula unit, similar to what has been found for the Bi-2201 compound.[14] This is a first clear indication that the tetragonal description is far from being realistic, and one should not entirely rely on it when comparing with ARPES or Raman experiments.

B. Fermi surface

Figure 2 depicts the cross cuts of the Fermi surface with the $k_z=0$ plane as calculated for the BCT cell. The contour plots have been obtained by associating a sharp Lorentzian to each eigenvalue and summing the contribution at the Fermi level from all the bands at each k point. Moving from the experimental structure [Fig. 2(a)] to the fully optimized structure [Fig. 2(b)] we observe small but visible changes in the Fermi surface topology. The two main barrels centered at X, arising from the Cu_d-O_p bands, giving rise to the well-known holelike Fermi surface, attain a more rounded shape and the splitting (usually indicated as ''bilayer splitting'') of the bonding and antibonding parts is generally reduced. Near the $\bar{M}$ point, where the splitting is expected to be larger, the interpretation is complicated by the hybridization with the BiO orbitals, which induces an anticrossing between the bands. Both BiO bands, with antibonding character and $p_{(x,y)}$ symmetry, are found to cross the Fermi level for the optimized structure, giving rise to two distinct intersecting pockets around $\bar{M}$, which dope the CuO_2 planes with additional holes. According to our calculations the structural optimization of BCT cell is therefore not sufficient to move the states with BiO character away from the Fermi level. This is in contrast with photoemission experiments where no clear evidence of BiO pockets is found around the $\bar{M}$ point, and with the nonmetallic character of the BiO plane as observed by scanning tunneling spectroscopy.[22]

Since photoemission and even more tunneling experiments probe only the surface layers of a material—and the BiO plane is the natural cleavage plane during the sample preparation—one might argue that the surface BiO bands might deviate from the bulk ones. We have therefore investigated this possibility and simulated the presence of a BiO plane terminated (001) surface. Thereby we used a slab-supercell technique which considers repeated slabs, each composed of two halves of BCT cells embedded in vacuum. The in-plane lattice constant was the one determined in the optimization of the bulk, while the atoms were allowed to relax along the direction perpendicular to the surface. Such relaxations were found to be of limited size, consistent with the highly two-dimensional nature of the compound, but still induced slight changes in the Fermi surface [see Fig. 2(c)]. The dimpling in the BiO plane doubles in value (from 0.09 to 0.16 Å) and the BiO bands becomes almost degenerate

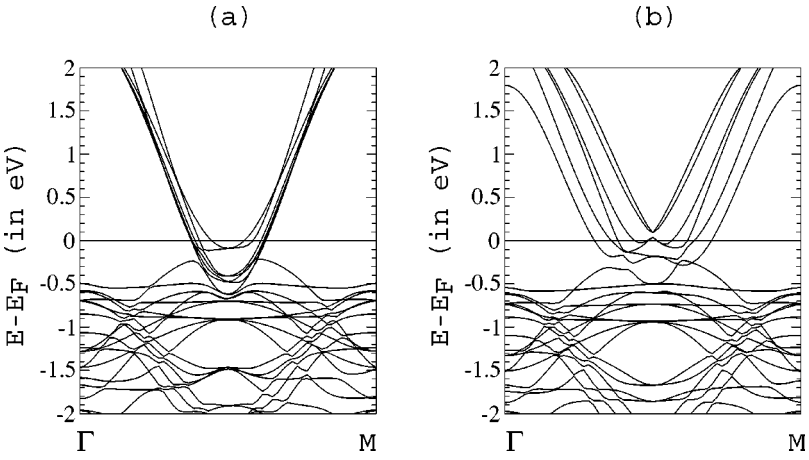

FIG. 3. Band structure of the undistorted (a) and distorted (b) orthorhombic cell along the $\Gamma-M$ direction in the orthorhombic Brillouin zone; the tetragonal $\bar{M}$ point lies in the middle of the $\Gamma-M$ line.

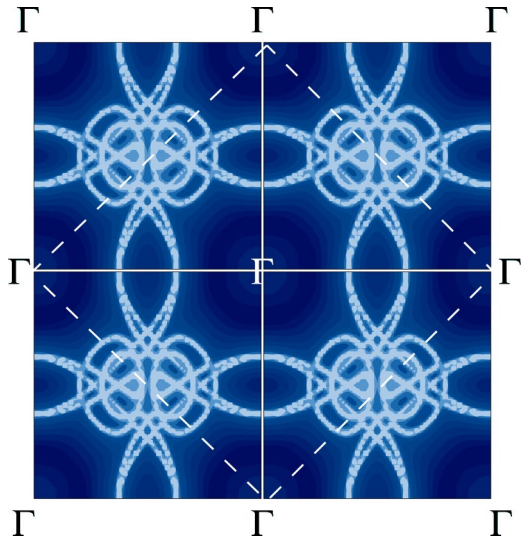

FIG. 4. (Color online) Fermi surface cross cuts in the k_x-k_y plane ($k_z=0$) for the AD-ORTH structure: the rotated square (dashed line) whose corners are the Γ point in the middle of the two axes compares with the tetragonal Brillouin zones shown in Fig. 2.

crossing the Γ-$\bar{M}$ direction at the same point. The CuO barrels move towards the M point and the BiO pockets becomes less distinguishable. Overall, the so optimized Fermi surface compares better with ARPES measurement (see, for instance, Refs. 23–27 and 12).

The structural distortion in the BiO plane occurring in the *real* Bi-2202 may be an additional effect altering the dispersion of the BiO bands and possibly inducing an upward shift of the partially occupied BiO bands around the M point of the tetragonal Brillouin zone. We plot in Fig. 3 the band structure in the vicinity of the Fermi level for Bi-2212 in the BCT (a) and the AD-ORTH structure (b), along the $\bar{\Gamma}-M$ line of the orthorhombic Brillouin zone. The M two-dimensional (2D) symmetry point of the tetragonal cell sits in the middle of the $\Gamma-M$ line. Four among the six bands which cross the Fermi level stem from the BiO plane while the other two are the bilayer-splitted CuO bands mirrored across the zone boundaries due to the $X\rightarrow\Gamma$ folding. The distortion in the Bi-2212 does not sensibly move the BiO bands, neither does it visibly reduce the hybridization with the CuO bands.

As shown in Fig. 4 the overall topology of the Fermi surface is now more complicated, in qualitative agreement with photoemission experiments that, as already mentioned, show multiple CuO barrels assigned to the scattering of the photoemitted electron from the orthorhombic distorted BiO planes. The incommensurate and disordered nature of the distortion together with finite energy resolution of the spectrometers may be responsible of extra broadenings that might justify why many of the details of the Fermi surface are smeared out and do not result into clear features at the Fermi level.

C. Raman-active phonons

A rigorous test for the quality of any structural characterization is the calculation of the phonon frequencies, which gives a sensible account on how well the equilibrium positions as well as the bonding between the atoms are described.

The different symmetries of the structures we used to characterize the Bi-2212 crystal—which are described by different space groups, i.e. *I4/mmm* and *Bbmb*, respectively, for the tetragonal and orthorhombic cells—lead to different spectra. In a group-theoretical analysis of the *I4/mmm* tetragonal cell, 14 Raman-active ($q=0$) modes ($6A_{1g}+1B_{1g}+7E_g$) are predicted.[28] In addition, several other vibrations are expected to become Raman active in the orthogonal cell due to the distortion or folding at the Brillouin-zone edge.[29,30] Limiting ourselves to the vibrations which do not lower the symmetry of the crystal, a group-theoretical analysis of the *Bbmb* space group foretells a total of $12A_g$ modes in the AD-ORTH cell, which in a first approximation separates into seven vibrations along the c axis and five along the a axis (see Ref. 29 for details). Six among the seven c axis modes are those present also in the tetragonal cell, and they involve the collective motions of the Cu, Sr, Bi, O_{Sr}, and O_{Bi} atoms. An additional c-axis out-of-phase vibration of the two (now inequivalent) O_{Cu} atoms in the CuO_2 plane[31] arises in the orthorhombic cell, due to the distortion.

The frequencies of the six A_{1g} Raman-active modes and the 12 A_g modes in the BCT and AD-ORTH cell, respectively, are listed in Tables III and IV together with the corresponding eigenvectors. We first comment on the phonon spectrum obtained with the tetragonal cell. The reported eigenvectors allow us to attribute, as evidenced by bold characters in Table III, the six frequencies (in increasing order of eigenvalue) to the main vibrations of Bi, Cu, Sr, O_{Bi}, O_{Cu}, and O_{Sr}. As expected, the phonons associated to all the oxygen atoms assume the highest values. Moreover, the motion of the three oxygen atoms has a somewhat purer character, while the lower vibrations of the transition metal ions involve the in- and out-of-phase motion of more than one atom.

To which extent are these phonons influenced by the presence of the orthorhombic distortion? As can be inferred from Table IV all the in-phase vibrations except one keep their pure c-axis character, and attains a value close to its counterpart for the BCT cell. The two highest modes at 597 and 367 increase in the range of 10–20 cm^{-1}, while the Cu vibration diminishes by the same amount. The out-of-phase vibration of the oxygen atoms in the CuO_2 plane, not present in the tetragonal cell, attains a frequency of 210 cm^{-1}.

The alternate expansion and contraction of the Bi-O bonds occurring in the AD-ORTH structure along the distortion direction changes the nature of the bonds which involve atoms in the BiO plane. As a consequence the c-axis vibration of the O_{Bi} atom is found to strongly couple with the a-axis vibration of the apical O_{Sr} atoms. As a net result, the mode hardens by 60 cm^{-1} and attains a value of 289 cm^{-1}. In turn, the a-axis vibration of the O_{Sr} atom mixes strongly with the c-axis vibration of the O_{Bi} atom, and additionally with the a-axis vibration of the Sr atom, so that a second mixed a/c axis mode appears at 192 cm^{-1}. As a matter of fact, the latter mixed modes might be envisaged as a breathing of the atomic distances in the SrO plane whenever this plane is approached by the O_{Bi} atom during its c-axis vibra-

TABLE III. Frequencies ω (in cm^{-1}) and eigenvectors of the six A_{1g} c-axis modes in the BCT cell.

ω	Cu	Sr	Bi	O_{Cu}	O_{Sr}	O_{Bi}
576	0.03	0.02	−0.27	−0.19	**0.94**	0.09
356	0.05	0.27	0.05	**−0.94**	−0.19	0.03
233	0.00	−0.03	0.21	−0.06	0.14	**−0.96**
163	−0.33	**0.87**	−0.27	0.22	−0.03	−0.10
116	**−0.92**	−0.23	0.25	−0.12	0.07	0.08
50	−0.17	−0.34	**−0.86**	−0.11	−0.24	−0.21

tion. In addition to the modes with pure or mixed c-axis character there are four pure a-axis vibrations. The a-axis vibrations of the Bi and Sr atoms are found at 106 and 132 cm^{-1}, respectively. The in-plane vibration of the Cu atoms instead results to be much harder, at a frequency of 355 cm^{-1}, three times larger than the corresponding vibration along the c axis. The most interesting finding, as we will discuss below, is relative to the O_{Bi} a-axis vibration, which attains a frequency of 424 cm^{-1}, almost twice the value calculated for its c-axis vibration.

It is interesting to compare our theoretical findings with experimental data. We start the discussion by saying that while the frequencies of the measured phonon peaks agree reasonably well among experiments performed under similar conditions, their assignment has been by no means unique and varied sensibly among different groups. Experiments previous to 1996 disagree in fact with each other on the interpretation of phonons in the whole spectrum (see, for instance, Table I in Ref. 32, and reference therein). In order to keep the discussion manageable, only the data obtained after 1996 will be considered. The strongest debate concerns the origin of the two highest frequencies, i.e., at around 460 and 630 cm^{-1}, which were attributed to the motion of the O_{Bi} and O_{Sr} atoms,[32–36] or vice versa.[37] Our calculations, both for the tetragonal and orthorhombic cells, give a strong support to the former type of attribution. Nevertheless, if the calculated value for the O_{Sr} mode is reasonably close to the experimental one, a striking deviation is found for the c-axis vibration of O_{Bi} (233 cm^{-1} for the tetragonal cell vs the experimental attributed value of 460 cm^{-1}). The introduction of the orthorhombic distortion, although strengthening this mode to around 290 cm^{-1}, does not improve sensibly the situation. Instead, we find that it is the a-axis vibration of the O_{Bi} atom to have a frequency of 424 cm^{-1}, close to the experimental peak. It is important to recall that all the modes we are discussing have A_g symmetry and are thus expected to appear in Raman spectra taken under noncrossed polarization geometry such as zz, xx, or yy. In light of these results, we associate the experimental peak around 460 cm^{-1} to the a-axis rather than the c-axis vibration of the O_{Bi} atom. Calculations of Raman spectra under different scattering geometries might be able to address this issue in the future and allow for a direct comparison with the experimental spectra. Another peak is observed in experiments at around 404 cm^{-1}, and attributed to the motions along the c axis of the oxygen atom in the CuO plane; our value for the in-phase c-axis vibration frequency of the O_{Cu} atoms is of 366 cm^{-1}. Moving towards lower frequencies, the modes observed by experiments around 115 and 130–140 cm^{-1} are concordantly (by the various experimental groups) attributed to the vibrations of the Sr and Cu atoms along the c axis. We find instead that the vibration of the Cu atom takes place at lower frequency than the one of Sr. Fewer investigations focused onto the low-frequency part of the spectrum where the phonons of the heavier atom, i.e., Bi, should appear, and a

TABLE IV. Frequencies ω (in cm^{-1}) and eigenvectors of the 12 A_g modes in the AD-ORTH cell. The atoms vibrate along the c and a axes, as indicated.

ω	Cu c axis	Cu a axis	Sr c axis	Sr a axis	Bi c axis	Bi a axis	O^1_{Cu} c axis	O^2_{Cu} c axis	O_{Sr} c axis	O_{Sr} a axis	O_{Bi} c axis	O_{Bi} a axis
597	0.02	0.00	0.02	0.00	−0.25	−0.02	−0.09	−0.10	**0.95**	0.12	0.05	0.04
424	0.00	0.00	−0.03	0.01	0.00	−0.21	0.04	0.03	0.05	−0.06	−0.01	**−0.97**
367	−0.09	−0.28	−0.19	−0.03	−0.02	−0.01	**0.67**	**0.63**	0.12	0.08	−0.08	0.06
356	0.02	**−0.95**	0.06	−0.10	0.01	0.00	−0.12	−0.27	−0.04	0.03	0.01	−0.02
289	−0.01	−0.06	0.02	0.09	−0.22	0.16	0.02	0.12	0.00	**−0.65**	**0.69**	0.00
210	−0.02	0.10	0.00	0.09	−0.09	0.00	**0.65**	**−0.62**	−0.08	0.26	0.31	−0.02
192	−0.03	0.04	0.21	**−0.45**	−0.22	−0.14	−0.19	0.27	−0.15	**0.55**	**0.49**	−0.03
163	−0.30	−0.01	**0.88**	0.17	−0.17	0.06	0.13	0.07	−0.01	−0.07	−0.20	−0.03
132	−0.07	0.10	0.06	**−0.86**	0.08	0.15	0.18	−0.17	0.08	−0.33	−0.19	−0.01
106	−0.41	0.01	−0.07	−0.04	0.02	**−0.86**	−0.01	−0.08	0.01	−0.20	0.03	0.20
104	**0.84**	0.00	0.22	−0.04	−0.22	−0.37	0.14	0.03	−0.05	−0.14	−0.11	0.09
47	0.16	0.00	0.28	0.01	**0.86**	−0.08	0.06	0.07	0.21	0.02	0.29	0.02

well-resolved peak at around 60 cm^{-1} has been successfully observed.[38–40] This is nicely in agreement with our calculated value of around 50 cm^{-1}. To summarize, a reasonable but not completely satisfactory agreement is obtained therefore only for the three phonons stemming from the Bi, O_{Cu}, and O_{Sr} atoms, which are found to be at most 10% weaker than their experimental counterparts; such underestimation, although at a smaller level, has been already observed for other high-T_c cuprate compounds.[13,41]

We must say that the experimental attribution of the peaks of a Raman spectra have been achieved either by investigating the change in frequency and/or intensity upon substitution with Y or Pb atoms, or by isotopes,[36] or by comparing with existent theoretical calculations. For the former type of analysis, the attribution strongly depends on the choice of the atomic site where the substitution is believed to take place, and therefore is not unambiguous. For what concerns the theory, the only calculations present in the literature have been performed by means of lattice-dynamics models by Prade *et al.*,[42] whose calculated frequencies are at 87, 164, 182, 387, 493, and 517 cm^{-1}. A thorough comparison of the phonon attribution given by Prade *et al.* with our results is not possible, because no eigenvectors are reported in their work. Moreover, such type of calculations rely on rather crude parametrizations of the interatomic potentials used to model the bonds, which their adequacy for a quantitative comparison with experiments.

V. CONCLUSIONS

We have performed extensive first-principles calculations for the electronic structure of the two-layer bismuth cuprate Bi-2212 focussing on the role of the structural arrangement. We have determined fully optimized atomic positions of three different structures, a body-centered tetragonal cell, with and without surface termination, and an averagely distorted orthorhombic structure simulating the observed incommensurate superstructure. We find that just the structural optimization of the body-centered tetragonal cell—leading to a volume reduction and to an increase in the c/a ratio—is sufficient to induce appreciable modifications in the shape of the Fermi surface that compare better with what has been measured by photoemission experiments; this is even more so after the inclusion of surface termination. Only within the orthorhombic distorted cell it is possible to reproduce the secondary structures observed in photoemission spectra.

The presence of BiO derived bands cutting the Fermi energy is a characteristic of all the band calculations we have performed, assuming both optimized, nonoptimized, and ideal and distorted geometries. Even an explicit treatment of correlation effects in the CuO_2 plane beyond the mean field[43] seems not to modify this picture leaving the hybridization between Cu and BiO bands unaltered. The nonmetallic character of BiO planes deduced by scanning tunneling spectroscopy and apparently confirmed by the absence of clear BiO derived structures in measured Fermi surfaces remains then a puzzling issue.

Ab initio calculation of phonon frequencies for ideal and distorted structures demonstrate clearly that the distortions have large effects and should be taken into account when interpreting Raman-scattering experiments. The symmetry lowering associated to the distortion makes more vibrations Raman active. Moreover, we have been able to make an alternative attribution of some specific vibrations. The final assignment of all the phonon frequencies would benefit from calculations of Raman spectra under different scattering geometries.

ACKNOWLEDGMENTS

We are grateful to E. Ya. Sherman for fruitful discussions on phonon frequencies. This work was partly funded by MIUR-''Progetto Giovani Ricercatori,'' and benefitted from support by the Austrian Science Fund (FWF, Project No. P13430) and the EU RTN network EXCITING, Contract No. HPRN-2002-00317. The computer facilities were granted by an INFM project ''Iniziativa Trasversale Calcolo Parallelo'' at the CINECA supercomputing center.

*Corresponding author. Email address: bellini.valerio@unimore.it

[1] D.M. Ori, A. Goldoni, U. del Pennino, and F. Parmigiani, Phys. Rev. B **52**, 3727 (1995).
[2] A.A. Levin, Yu. I. Smolin, and Yu. F. Shepelev, J. Phys.: Condens. Matter **6**, 3539 (1994).
[3] P.A. Miles, S.J. Kennedy, G.J. McIntyre, G.D. Gu, G.J. Russell, and N. Koshizuka, Physica C **294**, 275 (1998).
[4] J. Etrillard, P. Bourges, and C.T. Lin, Phys. Rev. B **62**, 150 (2000).
[5] S. Monastra, F. Manghi, and C. Ambrosch-Draxl, Phys. Rev. B **64**, 020507 (2001).
[6] S. Massidda, J. Yu, and A.J. Freeman, Physica C **152**, 251 (1988).
[7] H. Krakauer and W.E. Pickett, Phys. Rev. Lett. **60**, 1665 (1988).
[8] M.S. Hybertsen and L.F. Mattheiss, Phys. Rev. Lett. **60**, 1661 (1988).
[9] B. Szpunar and V.H. Smith Jr., Phys. Rev. B **45**, 10 616 (1992).
[10] H. Ding, A.F. Bellman, J.C. Campuzano, M. Randeria, M.R. Norman, T. Yokoya, T. Takahashi, H. Katayama-Yoshida, T. Mochiku, K. Kadowaki, G. Jennings, and G.P. Brivio, Phys. Rev. Lett. **76**, 1533 (1996).
[11] A. Bansil and M. Lindroos, Phys. Rev. Lett. **83**, 5154 (1999).
[12] M.C. Asensio, J. Avila, L. Roca, A. Tejeda, G.D. Gu, M. Lindroos, R.S. Markiewicz, and A. Bansil, Phys. Rev. B **67**, 014519 (2003).
[13] R. Kouba, C. Ambrosch-Draxl, and B. Zangger, Phys. Rev. B **60**, 9321 (1999).
[14] D.J. Singh and W.E. Pickett, Phys. Rev. B **51**, 3128 (1995).
[15] A. Lanzara, P.V. Bogdanov, X.J. Zhou, S.A. Kellar, D.L. Feng, E.D. Lu, T. Yoshida, H. Eisaki, A. Fujimori, K. Kishio, J.-I. Shimoyama, T. Noda, S. Uchida, Z. Hussain, and Z.-X. Shen, Nature (London) **412**, 510 (2001).
[16] O.K. Andersen, Phys. Rev. B **12**, 3060 (1975).
[17] D. J. Singh, *Plane waves Pseudopotentials and the LAPW Method* (Kluwer Academic, Dordrecht, 1994).
[18] P. Blaha, K. Schwarz, G. Madsen, D. Kvasnicka, and J. Luitz, Computer code WIEN2K (Karlheinz Schwarz, Technische Universität Wien, Austria, 1999).

[19] S.A. Sunshine, T. Siegrist, L.F. Schneemeyer, D.W. Murphy, R.J. Cava, B. Batlogg, R.B. van Dover, R.M. Fleming, S.H. Glarum, and S. Nakahara, Phys. Rev. B **38**, 893 (1988).
[20] O.K. Andersen, O. Jepsen, A.I. Lichtenstein, and I.I. Mazin, Phys. Rev. B **49**, 4145 (1994).
[21] R.S. Markiewicz, J. Phys. Chem. Solids **58**, 1179 (1997).
[22] M. Tanaka, Science **339**, 691 (1989).
[23] P. Aebi, J. Osterwalder, P. Schwaller, L. Schlapbach, M. Shimoda, T. Mochiku, and K. Kadowaki, Phys. Rev. Lett. **72**, 2757 (1994).
[24] P.V. Bogdanov, A. Lanzara, X.J. Zhou, S.A. Kellar, D.L. Feng, E.D. Lu, H. Eisaki, J.-I. Shimoyama, K. Kishio, Z. Hussain, and Z.-X. Shen, Phys. Rev. B **64**, 180505 (2001).
[25] T. Sato, T. Kamiyama, T. Takahashi, J. Mesot, A. Kaminski, J.C. Campuzano, H.M. Fretwell, T. Takeuchi, H. Ding, I. Chong, T. Terashima, and M. Takano, Phys. Rev. B **64**, 054502 (2001).
[26] D.L. Feng, C. Kim, H. Eisaki, D.H. Lu, A. Damascelli, K.M. Shen, F. Ronning, N.P. Armitage, N. Kaneko, M. Greven, J.-I. Shimoyama, K. Kishio, R. Yoshizaki, G.D. Gue, and Z.-X. Shen, Phys. Rev. B **65**, 220501 (2002).
[27] A.A. Kordyuk, S.V. Borisenko, M.S. Golden, S. Legner, K.A. Nenkov, M. Knupfer, J. Fink, H. Berger, L. Forró, and R. Follath, Phys. Rev. B **66**, 014502 (2002).
[28] The A_1g modes are symmetric *c*-axis vibration of Bi, Sr, Cu, O_{Bi}, O_{Sr}, and O_{Cu} atoms, the B_1g phonon is the out-of-phase motion of the O_{Cu} atoms also along the *c* axis, and E_g vibrations are planar *ab* displacements.
[29] S. Sugai and M. Sato, Jpn. J. Appl. Phys., Part 1 **28**, L1361 (1989).
[30] R. Liu, M.V. Klein, P.D. Han, and D.A. Payne, Phys. Rev. B **45**, 7392 (1992).
[31] Note that the out-of-phase vibration of the O_{Cu} ions is much lower in frequency compared to its counterpart in YBCO. The reason for this should be ascribed to the fact that different displacement patterns are involved due to different point symmetries of the ions in the unit cells.
[32] M. Kakihana, M. Osada, M. Käll, L. Börjesson, H. Mazaki, H. Yasuoka, M. Yashima, and M. Yoshimura, Phys. Rev. B **53**, 11 796 (1996).
[33] X.H. Chen, K.Q. Ruan, G.G. Qian, S.Y. Li, L.Z. Cao, J. Zou, and C.Y. Xu, Phys. Rev. B **58**, 5868 (1998).
[34] M. Osada, M. Kakihana, H. Arashi, M. Käll, and L. Börjesson, Phys. Rev. B **59**, 8447 (1999).
[35] G.V.M. Williams, D.M. Pooke, D.J. Pringle, H.J. Trodahl, J.L. Tallon, J. Quilty, N. Malde, J.L. Macmanus-Driscoll, A. Crossley, and L.F. Cohen, Phys. Rev. B **62**, 1379 (2000).
[36] A.E. Pantoja, D.M. Pooke, H.J. Trodahl, and J.C. Irwin, Phys. Rev. B **58**, 5219 (1998).
[37] C. Kendziora, S.B. Qadri, and E. Skelton, Phys. Rev. B **56**, 14 717 (1997).
[38] M. Osada, M. Kakihana, K. Mikael, and L. Börjesson, J. Phys. Chem. Solids **59**, 2003 (1998).
[39] M. Boekholt, G. Güntherodt, and V.V. Moshchalkov, Physica C **192**, 191 (1992).
[40] J. Sapriel, J. Schneck, J.F. Scott, J.C. Tolédano, L. Pierre, J. Chavignon, C. Daguet, J.P. Chaminade, and H. Boyer, Phys. Rev. B **43**, 6259 (1991).
[41] T. Thonhauser and C. Ambrosch-Draxl, Phys. Rev. B **67**, 134508 (2003).
[42] J. Prade, A.D. Kulkarni, F.W. de Wette, U. Schröder, and W. Kress, Phys. Rev. B **39**, 2771 (1989).
[43] V. Bellini, C. Rozzi, and F. Manghi (unpublished).